Palmitoylation is a prerequisite for dimerization-dependent raftophilicity of rhodopsin

Keiji Seno[‡§] and ![ORCID] Fumio Hayashi[¶1]

From the ‡Department of Biology, Faculty of Medicine, and §International Mass Imaging Center, Hamamatsu University School of Medicine, 1-20-1 Handayama, Higashi-ku, Hamamatsu, Shizuoka 431-3192, Japan and the ¶Department of Biology, Graduate School of Science, Kobe University, 1-1 Rokkodai, Nada, Kobe 657-8501, Japan

Edited by Henrik G. Dohlman

The visual photopigment rhodopsin (Rh) is a prototypical G protein–coupled receptor (GPCR) responsible for initiation of the phototransduction cascade in rod photoreceptors. Similar to other GPCRs, Rh can form dimers or even higher oligomers and tends to have a supramolecular organization that is likely important in the dim light response. Rh also exhibits high affinity for lipid rafts (*i.e.* raftophilicity) upon light-dependent binding with the cognate G protein transducin (G_t), suggesting the presence of lipid raft-like domains in the retinal disk membrane and their importance in phototransduction. However, the relationship between Rh oligomerization and lipid rafts in the disk membrane remains to be explored. Given previous findings that G_t binds to dimeric Rh and that Rh is posttranslationally modified with two highly raftophilic palmitoyl moieties, we hypothesized that Rh becomes raftophilic upon dimerization. Here, using biochemical assays, we found that Rh*–G_t complexes in the detergent-resistant membrane are partially resistant to cholesterol depletion by methyl-β-cyclodextrin and that the Rh-to-G_t stoichiometry in this methyl-β-cyclodextrin–resistant complex is 2:1. Next, we found that IgG-mediated Rh–Rh cross-linking renders Rh highly raftophilic, supporting the premise that Rh becomes raftophilic upon dimerization. Rh depalmitoylation via reduction of thioester linkages blocked the translocation of IgG–cross-linked Rh to the detergent-resistant membrane, highlighting that the two palmitoyl moieties are important for the dimerization-dependent raftophilicity of Rh. These results indicate that palmitoylated GPCRs such as Rh can acquire raftophilicity upon G protein–stabilized dimerization and thereby organize receptor-cluster rafts by recruiting raftophilic lipids.

The visual photopigment rhodopsin (Rh)[2] is a prototypical member of the class A family of G protein–coupled receptors (GPCRs), the largest and most diverse group of membrane receptor proteins in eukaryotes. Rh is responsible for initiating the phototransduction cascade in photoreceptor cells. The phototransduction cascade involves collision coupling of receptors and the trimeric G protein transducin (G_t), which is freely diffusing in the retinal disk membrane stacked in rod photoreceptor outer segments (ROS) (1). Photoexcited Rh (Rh*) binds to and activates G_t, and the activated $G\alpha_t$ subunit is released to activate downstream signaling.

Accumulating evidence suggests that Rh has a propensity to form dimers, or even higher oligomers, in the disk membrane (2–6), similar to other GPCRs (7). For example, studies based on atomic force microscopy revealed that Rh can form paracrystalline arrays of Rh dimers (3, 8) or nano-sized domains centrally confined in the disk membrane (9). A cryoelectron tomographic study found static track-like arrays of Rh dimers in the murine disk membrane (6). Simulation studies of the kinetics of G_t activation have corroborated the hypothesis that supramolecular organization of Rh works as a signaling scaffold for G_t activation and enables rod photoreceptor cells to detect single photons (6, 10). Furthermore, molecular dynamics simulations showed that Rh has various dimerization interfaces through which Rh forms dimers and highly ordered arrays of Rh dimers (5). The dimerization interfaces were consistent with those observed in previous crystallographic studies (11) and a biochemical cross-linking study (12).

In addition to the heterogeneity resulting from Rh self-assembly, the disk membrane is likely a heterogeneous structure because of the presence of lipid raft-like microdomains. Although monomeric Rh is the favorable form in non-lipid raft microenvironments (*i.e.* raftophobic) (13, 14), we previously found that G_t translocates into the detergent-resistant membrane (DRM) when it forms a tight complex with Rh*, suggesting the high lipid raft affinity (raftophilicity) of the Rh*–G_t complex (15). Based on pioneering studies suggesting that the binding partner of G_t in the Rh*–G_t complex is the Rh dimer (4, 16), we speculate that Rh acquires high raftophilicity upon dimerization. In this regard, it is intriguing that Rh has two tandem cysteine residues (Cys-322 and Cys-323) that are posttranslationally modified with two palmitoyl moieties (17). Palmitoylation on multiple residues is known to be a strong lipid raft–targeting mechanism for transmembrane proteins (18). Although many studies have reported that the lipid microenvironment is important for the oligomerization and

[2] The abbreviations used are: Rh, rhodopsin; GPCR, G protein–coupled receptor; G_t, trimeric G protein transducin; ROS, rod outer segment(s); Rh*, photoexcited Rh (metarhodopsin II); DRM, detergent-resistant membrane; DSM, detergent-soluble membrane; GTPγS, guanosine 5′-3-O-(thio)triphosphate; L-DRM, DRM prepared from light-exposed ROS; D-DRM, DRM prepared from dark-adapted ROS; MCD, methyl-β-cyclodextrin; HA, hydroxylamine; CBB, Coomassie Brilliant Blue.
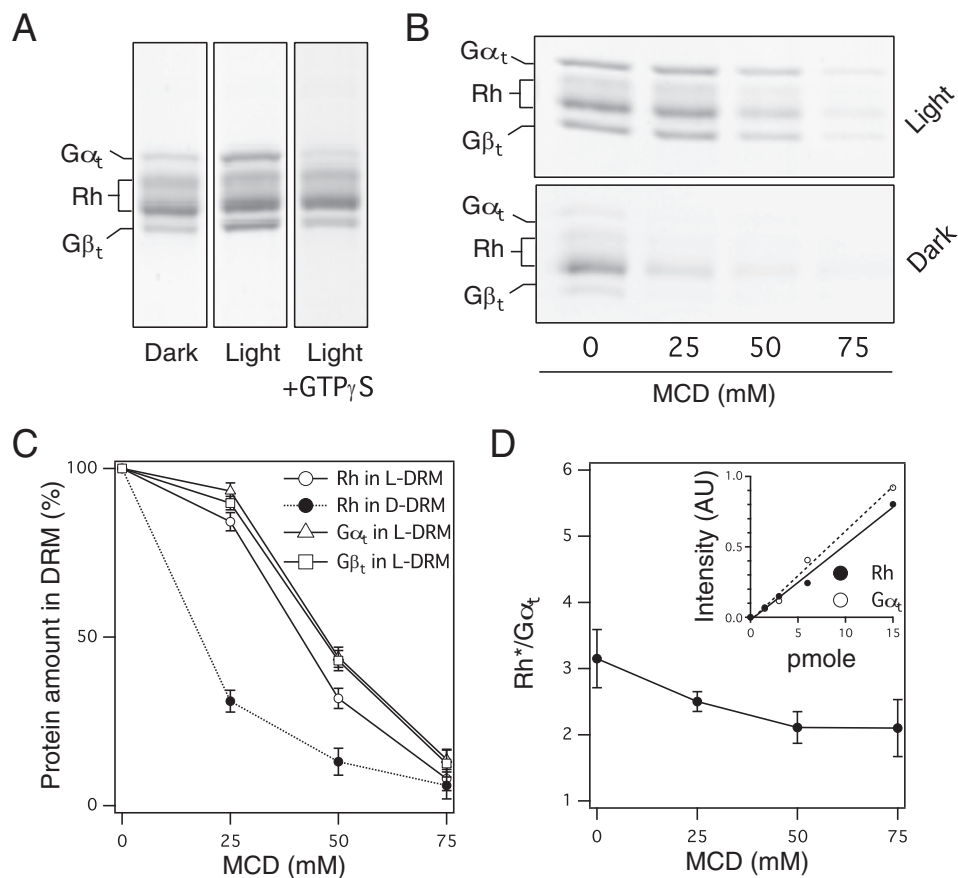
Figure 1. MCD-resistant raftophilicity of Rh*–G$_t$ complexes and binding stoichiometry. *A*, profiles of proteins recruited to the DRM of ROS under the indicated conditions. Proteins were stained with Coomassie Brilliant Blue (CBB). *Left*, DRM of dark-adapted ROS. *Center*, DRM of light-exposed ROS. *Right*, DRM of light-exposed and GTPγS-treated ROS. Bands of Gγ$_t$ are omitted. *B*, effect of MCD concentration on protein profiles in the DRM of light-exposed ROS (*top*) and dark-adapted ROS (*bottom*). GTP was absent. *C*, MCD concentration dependence of the amount of Rh, Gα$_t$, and Gβ$_t$ relative to that in the absence of MCD. Data were obtained by densitometric scanning of CBB-stained gels as shown in *B* and expressed as the mean ± S.D. of three experiments. *D*, effect of MCD concentration on the Rh/Gα$_t$ ratio in the DRM of light-exposed ROS without GTP. Data are expressed as the mean ± S.D. of three experiments. *Inset*, linear standard curves of purified Rh and Gα$_t$ obtained by densitometric scanning of CBB-stained gels. *AU*, arbitrary unit.

functioning of GPCRs (19), little is known about the oligomerization-dependent generation of raftophilic microdomains, with the exception of a study on the purinergic receptor (20).

Against this backdrop, we hypothesized that dimerization confers high raftophilicity to Rh. To test this, we examined whether the stoichiometric ratio between Rh and G$_t$ in the Rh*–G$_t$ complex within the DRM is 2:1. We also examined the raftophilicity of IgG–cross-linked Rh by assessing its translocation into the DRM. We found that the stabilized dimer of Rh, whether the binding partner is G$_t$ or IgG, exerts high raftophilicity. We also provide evidence for the importance of palmitoyl modifications in the oligomerization-dependent raftophilicity of this receptor.

Results

MCD-resistant raftophilicity and stoichiometry of Rh*–G$_t$ complexes

To assess the stoichiometric ratio between Rh and G$_t$ in Rh*–G$_t$ complexes, we obtained Rh*–G$_t$ complexes that are found in the DRM fraction of light-exposed frog disk membranes. In the absence of GTP, G$_t$ translocates from the detergent-soluble membrane fraction (DSM) to the DRM fraction in a light-depen-

dent manner (Fig. 1*A*). The translocation can be reversed by addition of GTPγS, an unhydrolyzable analog of GTP (15) (Fig. 1*A*), suggesting that the translocation likely occurs because of the high raftophilicity of the Rh*–G$_t$ complex.

The recruitment of Rh* and G$_t$ to the DRM of light-exposed ROS (L-DRM) is highly resistant to cholesterol depletion of disks by methyl-β-cyclodextrin (MCD) prior to cold detergent treatment (Fig. 1*B*). Rh residing in the DRM of dark-adapted ROS (D-DRM) was easily removed by MCD, whereas Rh* and G$_t$ in L-DRM were resistant to MCD (Fig. 1*B*, compare *top* and *bottom*).

We next measured the amounts of Rh and G$_t$ (Gα$_t$ and Gβ$_t$) in the DRM by densitometric scanning of Coomassie Brilliant Blue–stained protein bands using highly purified proteins as standards. MCD dose dependence curves showed that Rh* and G$_t$ in the L-DRM are considerably resistant to MCD (ED$_{50}$, about 45 mM), whereas Rh in the D-DRM is susceptible to MCD (ED$_{50}$, about 20 mM) (Fig. 1*C*). Prior to MCD treatment of ROS, the ratio between Rh* and G$_t$ in the L-DRM was ∼3:1 or more (Fig. 1*D*). This ratio converged to 2:1 as the concentration of MCD increased (Fig. 1*D*). This result suggests that the stoichiometry of the MCD-resistant Rh*–G$_t$ complex is 2:1 and that
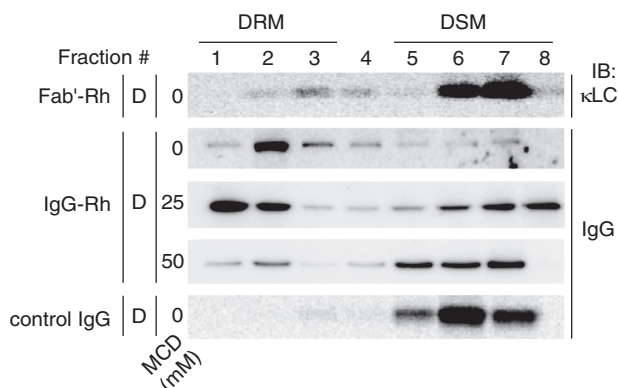
Figure 2. Raftophilicity of IgG– cross-linked Rh. Distribution of IgG– cross-linked Rh and Rh bound to Fab' fragments of the same antibody in the DRM and DSM of dark-adapted ROS membranes. The Rh-specific monoclonal antibody IgG-1D4 and its Fab' fragment were detected by immunoblotting (*IB*) with an anti-mouse IgG antibody and anti-mouse κ-light chain antibody, respectively. Prior to DRM preparation, ROS membranes were treated with varying concentrations of MCD, as indicated.

extra Rh is recruited by Rh*–G$_t$ in the L-DRM of ROS not treated with MCD.

Dimerization renders Rh raftophilic

To confirm that dimerization renders Rh raftophilic, we examined the effect of IgG cross-linking on the distribution of Rh in the DRM (Fig. 2). When Rh in the ROS membrane was incubated with a monovalent probe, *i.e.* the Fab' fragment of the monoclonal antibody 1D4 raised against the carboxyl terminus of Rh (21), the major population of Rh–Fab' complexes was distributed in the DSM. In contrast, when Rh was cross-linked with IgG of the same antibody, cross-linked-Rh was preferentially recruited to the DRM (Fig. 2). Recruitment of IgG– cross-linked Rh to the DRM was considerably resistant to cholesterol depletion by MCD, although recruitment was almost completely suppressed at 50 mM MCD (Fig. 2).

Palmitoylation is essential for the dimerization-dependent raftophilicity of Rh

We next confirmed the importance of palmitoyl moieties in the dimerization-dependent raftophilicity of Rh. Rh molecules in ROS membranes were depalmitoylated by reduction with 20 mM DTT, and completion of the reaction was monitored by MALDI-TOF MS. The masses of tryptic peptides were obtainable from the carboxyl-terminal portion of bullfrog Rh and were predicted by ExPasy, the bioinformatics resource portal of the Swiss Institute of Bioinformatics (Fig. 3*A*). When ROS membranes were not treated with DTT, doubly palmitoylated tryptic peptides were observed (Fig. 3*B*, *top panel*). After DTT treatment, palmitoylated peptides were undetectable (Fig. 3*B*, *bottom panel*). We further examined the effect of depalmitoylation by 20 mM DTT or 1 M neutral hydroxylamine (HA) on the translocation of IgG– cross-linked Rh to the DRM and found that depalmitoylated Rh preferentially resides in the DSM even when cross-linked with IgG, whereas cross-linked native Rh exclusively resides in the DRM (Fig. 4).

Discussion

In this study, we found that doubly palmitoylated Rh gains strong raftophilicity upon dimerization. This finding revealed that the two types of membrane heterogeneity in the retinal disk membrane, *i.e.* heterogeneity based on self-assembly of Rh and self-organization of lipid raft–like membrane domains, are interdependent and inseparable from each other. We also found that palmitoylation is indispensable for the dimerization-induced raftophilicity of GPCRs. Although numerous studies have implied the importance of the lipid microenvironment for GPCR oligomerization (19), very little is known about the dimerization-dependent raftophilicity of GPCRs and its relationship with palmitoylation, with the exception of a study on the purinergic receptor (20). Our results contribute to a deeper understanding of the signal transduction mechanisms of many palmitoylated GPCRs, which rely on oligomerization and localization to lipid rafts to function (7, 19).

We and others have reported previously that Rh*–G$_t$ complexes that form in a light-dependent manner in the absence of GTP preferentially distribute in the L-DRM of ROS membranes, suggesting their high raftophilicity (15, 22, 23). Here we discovered that the raftophilicity of the complex is resistant to cholesterol depletion by MCD. Upon increasing the concentration of MCD used to pretreat bleached ROS membranes, the Rh*/Gα_t ratio in the L-DRM asymptotically decreased to about 2 (Fig. 1*D*). This suggests that the complex is considerably resistant to MCD and that the binding partner of G$_t$ in the complex is the Rh dimer. This stoichiometric ratio was in agreement with previous studies of the Rh*–Gα_t complex, purified using a mild detergent and affinity chromatography (24–26). Taken together with previous reports, our findings suggest that the membrane-spanning region of the raftophilic Rh*–Gα_t complex is the G$_t$-stabilized Rh* dimer and that dimeric Rh is raftophilic in the disk membrane. This hypothesis was corroborated by demonstrating the raftophilicity of IgG– cross-linked Rh and its resistance to cholesterol depletion by MCD (Fig. 2). Although the premise that IgG promotes Rh dimerization has not been strictly proven, the distinctive difference between Rh bound by monovalent Fab' and divalent IgG in both raftophilicity and MCD tolerance suggests the ability of IgG-1D4 to promote Rh dimerization. The tolerance of the raftophilicity of the Rh dimer (stabilized either by G$_t$ or IgG) to cholesterol depletion indicates that the interaction between the two Rh molecules is purely a protein–protein interaction rather than involving lipidic elements or, alternatively, reflects the intercalation of cholesterols between the two Rh molecules, which could hinder the activity of MCD on cholesterol. Furthermore, G$_t$ bound to the cytoplasmic surface of the Rh dimer as well as the recruitment of raftophilic lipids other than cholesterol, *e.g.* disaturated phospholipids rich in retinal disks (27), to the vicinity of the dimerization interface can also shield cholesterol from MCD.

We found that depalmitoylated Rh is not raftophilic even after dimerization (Fig. 4), indicating that palmitoyl moieties are crucial for the dimerization-dependent raftophilicity of Rh. This result is consistent with previous findings that palmitoylation of GPCRs plays a role in the compartmentalization of many GPCRs (*e.g.* the serotonin 5HT$_{1A}$ receptor (28) and μ-opioid receptor (29)) and their oligomers into raftophilic membrane nanodomains in a cholesterol-dependent manner (19). Based on our findings and accumulating evidence, we con-

A

```
         250        260        270        280        290        300
ATTQKAEKEV TRMVVIMVIF FLICWVPYAY VAFYIFTHQG SEFGPIFMTV PAFFAKSSAI

         310        320        330        340        350
YNPVIYIMLN KQFRNCMITT LCCGKNPFGD EDASSAATSK TEATSVSTSQ VSPA
```

N$_{315}$~K$_{340}$+2 palmitoyl +1 carbamidomethyl   3197.6216

N$_{315}$~K$_{325}$+0 palmitoyl +3 carbamidomethyl   1357.5731

N$_{326}$~K$_{340}$ 1496.6499

B

No DTT

3197.6
N$_{315}$~K$_{340}$+2 palmitoyl +1 carbamidomethyl

1496.6
N$_{326}$~K$_{340}$

DTT 10 hours

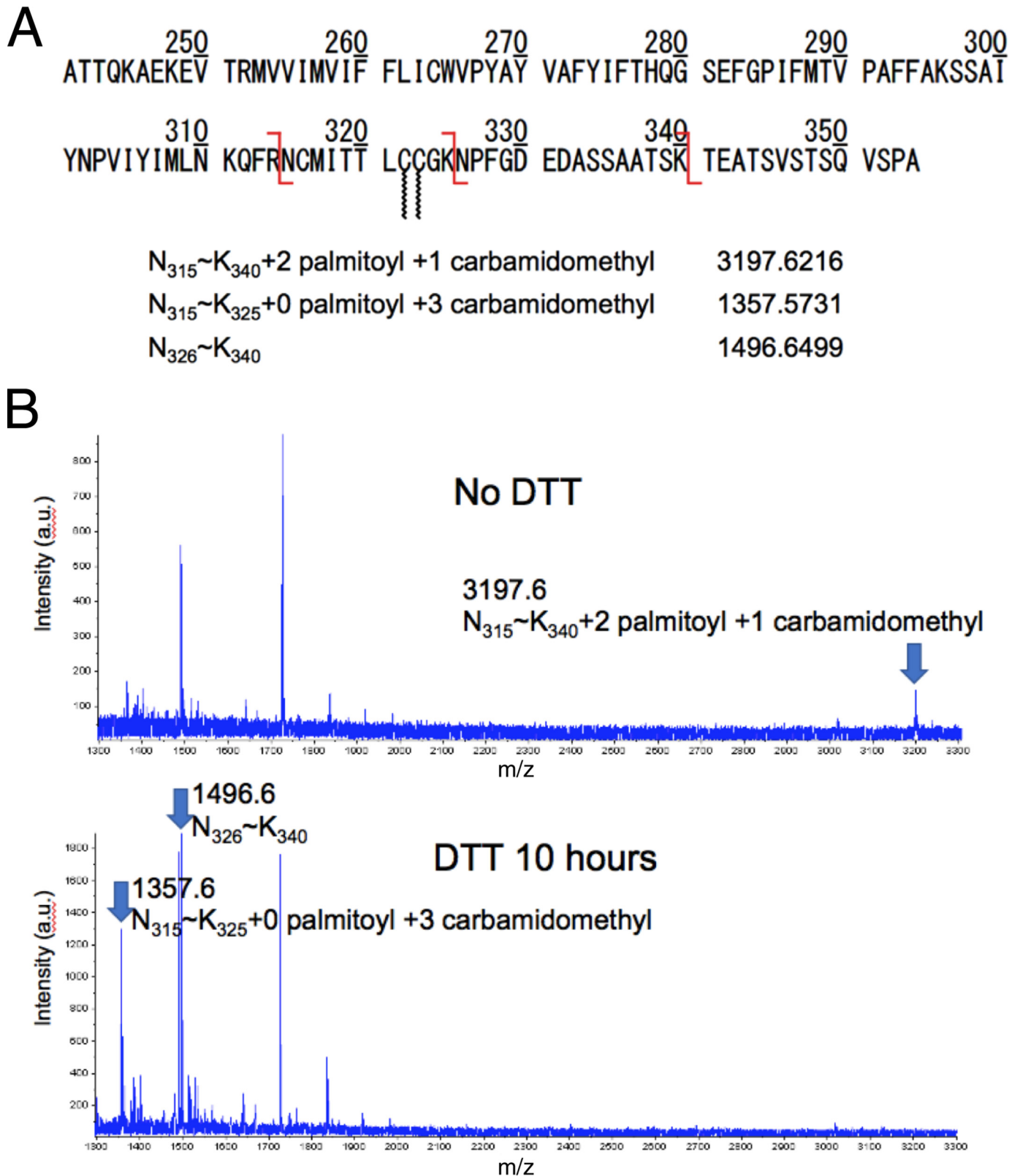1357.6
N$_{315}$~K$_{325}$+0 palmitoyl +3 carbamidomethyl

Figure 3. Depalmitoylation of Rh confirmed by MALDI-TOF MS. *A*, C-terminal 114 amino acid sequence of bullfrog Rh (*top*). Palmitoylated cysteine residues are indicated by the *jagged line*s. Trypsin digestion sites around the palmitoylation sites are indicated by *red lines*. Predictable peptide mass figures were calculated based on results from the bioinformatics resource portal of the Swiss Institute of Bioinformatics (51) (http://web.expasy.org/peptide_mass/) (*bottom*). *B*, representative result of MALDI-TOF MS of digested Rh peptides before and after reduction of thioester linkages with 20 mM DTT.

clude that dimerization bestows high raftophilicity to Rh and that palmitoyl modifications to Rh are crucial for dimerization-dependent raftophilicity.

The requirement of palmitoyl modifications for raft affinity of dimeric Rh hints at why Rh becomes raftophilic upon dimerization. When considering Rh dimerization, it should be
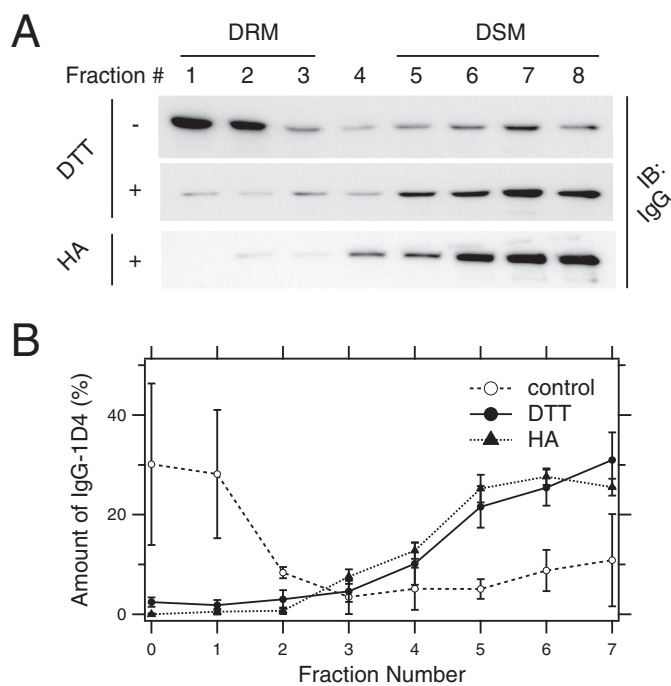
Figure 4. Effect of depalmitoylation on the distribution of IgG–cross-linked Rh to DRM. *A*, distribution of IgG-1D4 bound to Rh in the DRM and DSM of ROS membranes before (*top*) and after (*bottom*) depalmitoylation with 20 mm DTT or 1 m neutral HA. Representative immunoblot (*IB*) images are shown. *B*, quantitation of IgG-1D4. Data are expressed as the mean ± S.D. of three experiments.

Figure 5. Structure of the Rh homodimer via the H1–H8 interface. The homodimer of palmitoylated Rh was modeled according to the crystal structure of bovine Rh in trigonal form (PDB code 1GZM) (49). *A*, the two monomers in the asymmetric unit contacting through the H1–H8 interface are viewed from the cytoplasmic surface of the disk membrane. The dimer is placed so that the palmitoyl modifications are aligned vertically. *B*, the side view of a dimer. These models were created with Deep View Swiss-Pdb Viewer (http://spdbv.vital-it.ch/) (50). (Please note that the JBC is not responsible for the long-term archiving and maintenance of this site or any other third party hosted site.)

noted that the Rh monomer is anisotropic in the raftophilicity of its membrane-spanning surface. Although monomeric Rh is non-raftophilic (raftophobic) in nature (13, 14), the Rh molecule is modified with two palmitoyl moieties (30), which are known to be a raft-targeting mechanism for transmembrane proteins (18). These modifications at the tip of juxtamembrane helix 8 (H8) insert into the membrane and would provide a raftophilic singular area to the membrane-spanning surface of H8 facing the cytoplasmic leaflet of the disk lipid bilayer. If we assume that Rh forms a dimer through the dimerization interface constituted by helix 1 and H8 (H1–H8-H1–H8 interface), as proposed by studies based on electron microscopy (31, 32), crystallography (11, 33, 34), chemical cross-linking (12), and coarse-grained molecular dynamics simulation (5), then the palmitoyl modifications would be exposed at both edges of the dimerization interface (Fig. 5). On the other hand, the dimerization interface of a Rh molecule is covered by the other Rh molecule. Thus, upon dimerization, the ratio between the area covered by the raftophilic palmitoyl modifications and the raftophobic surface excluded by the dimerization interface of each Rh would increase. The discontinuous increase in this ratio may render Rh raftophilic when it forms a dimer.

Determining the functional role of dimerization-dependent raftophilicity of Rh in the phototransduction system is beyond the scope of this study. However, our findings provide hints regarding why Rh tends to form paracrystalline arrays of Rh dimers, as observed by electron microscopy and atomic force microscopy (2, 3, 8, 35). Although Rh dimerization is based on protein–protein interactions, it can be presumed that recruitment of raftophilic lipids to the vicinity of the Rh dimer stabi-
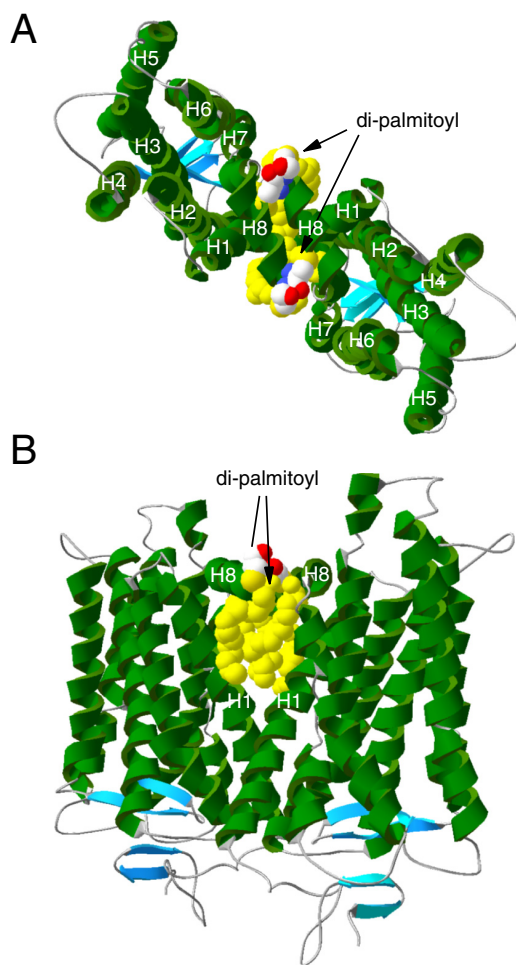
lizes the raftophilic Rh dimer and, thereby, stabilizes its higher oligomer. In this context, it is intriguing that the phototransduction machinery in the rod outer segment has a strong efficacy gradient along the longitudinal axis, *i.e.* the base of ROS can respond to light more efficiently than the tip (36). Given that basal disks have a higher cholesterol content than tip disks (37), the higher efficacy of the phototransduction system at the base can be explained by the stabilization of higher-order oligomers of Rh by cholesterol in basal disks. Although this hypothesis is arguable (36), it remains to be tested. In addition, the dimerization-dependent raftophilicity of Rh may contribute to enhancing the efficacy of rod photoreceptors by recruiting the Rh kinase inhibitor recoverin (S-modulin in frogs (38)). It has been reported that the dim flash response is suppressed in photoreceptors expressing palmitate-deficient rhodopsin (39). This effect of depalmitoylation has been attributed to the disinhibition of Rh phosphorylation (39). Consistent with this hypothesis, recoverin is known to work efficiently in raftophilic

environments (40). Thus, the dimerization-dependent raftophilicity of palmitoylated Rh is advantageous for efficient suppression of Rh* phosphorylation. Indeed, palmitoylation and levels of phosphorylation appear to be correlated in GPCRs in general (41). These results collectively suggest that dimerization-dependent raftophilicity plays an important role in the regulation of palmitoylated GPCRs.

Experimental procedures

Materials

This study was approved by the Institutional Animal Care and Use Committee and carried out according to Kobe University animal experimentation regulations. All experiments described were carried out using frogs (*Rana catesbeiana*). The mouse monoclonal anti-Rh antibody (1D4) was purchased from the University of British Colombia via Flintbox. Other antibodies were purchased from GE Healthcare. $G\alpha_t$, $G\beta\gamma_t$, and urea-washed ROS membranes were prepared from frog retina (42). Highly purified Rh was obtained as described previously (43).

Preparation of ROS

ROS were prepared from dark-adapted frogs (*R. catesbeiana*) by the sucrose flotation method (44). Membranes were suspended in isotonic buffer A (100 mM Tris-HCl, 5 mM MgCl$_2$, 5 mM dithiothreitol, and 0.2 mM phenylmethylsulfonyl fluoride (pH 7.5)). Rh concentration was calculated from absorbance at 504 nm based on the molecular extinction coefficient of Rh ($\epsilon = 4.06 \times 10^4$) (45). Aliquots of ROS suspension (200 nmol Rh) were stored at -80 °C in lightproof plastic tubes.

DRM preparation

An aliquot of ROS membrane suspension in buffer A containing 0.3 mg of Rh (about 10 nmol) was centrifuged at $10,000 \times g$ for 5 min at 4 °C. The pellet was solubilized with 56 μl of buffer A containing 1% Triton X-100. After addition of sucrose (final concentration, 0.9 M), the sample was overlaid with 60 μl each of 0.8 and 0.5 M sucrose and centrifuged at $436,000 \times g$ for 30 min at 0 °C. Fractions (30 μl) were collected from the top of the tube downward and stored at 0 °C. DRM was obtained from fractions 1–3. Quantitative determination of Rh and $G\alpha_t$ in the samples was performed by densitometric scanning of a Coomassie Brilliant Blue–stained SDS-PAGE gel using ImageJ software and purified Rh and $G\alpha_t$ as standards. To obtain good separation between $G\alpha_t$ and $G\beta_t$ from Rh, we used 12.5% Perfect NT Gel M purchased from D.R.C. Co. Ltd. (Tokyo, Japan). The concentrations of Rh and $G\alpha_t$ in the standard samples were determined using spectrophotometric data (absorbance at 500 and 280 nm, respectively) and molar extinction coefficients of Rh and $G\alpha_t$ (46) ($\epsilon = 3.04 \times 10^4$).

IgG cross-linking of Rh

Dark-adapted ROS membranes (0.3 mg suspended in 50 μl buffer A) were incubated with 10 μg of IgG-1D4 for 1 h at 0 °C in the dark. The molar ratio between Rh and IgG was roughly 130:1.

Depalmitoylation of Rh

Depalmitoylation was performed with DTT (47) or neutral HA (48). Briefly, in the case of DTT, ROS membranes were incubated with buffer B (10 mM HEPES, 98 mM potassium gluconate, 2.5 mM KCl, and 2 mM MgCl$_2$ (pH 8.6)) containing 20 mM DTT for 10 h at room temperature in the dark. In the case of HA, ROS membranes were incubated with buffer C (10 mM Tris, 2 mM MgCl$_2$, 20 mM NaCl, and proteinase inhibitor mixture (pH 7.9)) containing 1 M hydroxylamine (pH was adjusted to 7.9) for 0.5 h at 37 °C in the dark. After the treatments, membranes were washed three times with buffer B by centrifugation at $100,000 \times g$ for 5 min at 4 °C.

Mass spectrometric determination of Rh depalmitoylation

ROS membranes containing 70 μg of Rh with or without DTT treatment were washed by suspension in 1 ml of buffer D (10 mM Tris-HCl, 5 mM tris(2-carboxyethyl)phosphine, 1 mM EGTA, and 0.1 mM phenylmethylsulfonyl fluoride (pH 7.5)) and centrifugation at $436,000 \times g$ for 5 min. Proteins in the pellets were reduced by suspending and incubating for 1 h with buffer E (50 mM Tris-HCl, 20 mM iodoacetamide, and 1 mM EGTA (pH 7.5)) at room temperature. The samples were then centrifuged at $436,000 \times g$ for 5 min. Pellets were solubilized with 23 μl of 1% octylglucoside containing 25 mM ammonium hydrogen carbonate. The samples were digested by adding 1.4 μg of l-1-tosylamido-2-phenylethyl chloromethyl ketone trypsin and incubating overnight at 37 °C. After digestion, the samples were diluted 10-fold by distilled water, and 2-μl aliquots of the samples were mixed with 2 μl of matrix solution (50% methanol, 2% 2,5-dihydroxybenzoic acid, and 0.1% trifluoroacetic acid). 1 μl of each mixture was deposited on an MS target plate. MS analyses were performed using a quadrupole TOF-type mass spectrometer (QSTAR Elite, AB Sciex).

References

1. Pugh, E. N., Jr., and Lamb, T. D. (1993) Amplification and kinetics of the activation steps in phototransduction. *Biochim. Biophys. Acta.* **1141,** 111–149
2. Corless, J. M., McCaslin, D. R., and Scott, B. L. (1982) Two-dimensional rhodopsin crystals from disk membranes of frog retinal rod outer segments. *Proc. Natl. Acad. Sci. U.S.A.* **79,** 1116–1120
3. Fotiadis, D., Liang, Y., Filipek, S., Saperstein, D. A., Engel, A., and Palczewski, K. (2003) Atomic-force microscopy: Rhodopsin dimers in native disc membranes. *Nature* **421,** 127–128
4. Jastrzebska, B., Tsybovsky, Y., and Palczewski, K. (2010) Complexes between photoactivated rhodopsin and transducin: progress and questions. *Biochem. J.* **428,** 1–10
5. Periole, X., Knepp, A. M., Sakmar, T. P., Marrink, S. J., and Huber, T. (2012) Structural determinants of the supramolecular organization of

G protein-coupled receptors in bilayers. *J. Am. Chem. Soc.* **134,** 10959–10965

6. Gunkel, M., Schöneberg, J., Alkhaldi, W., Irsen, S., Noé, F., Kaupp, U. B., and Al-Amoudi, A. (2015) Higher-order architecture of rhodopsin in intact photoreceptors and its implication for phototransduction kinetics. *Structure* **23,** 628–638

7. Angers, S., Salahpour, A., and Bouvier, M. (2001) Dimerization: an emerging concept for G protein-coupled receptor ontogeny and function. *Annu. Rev. Pharmacol. Toxicol.* **42,** 409–435

8. Liang, Y., Fotiadis, D., Filipek, S., Saperstein, D. A., Palczewski, K., and Engel, A. (2003) Organization of the G protein-coupled receptors rhodopsin and opsin in native membranes. *J. Biol. Chem.* **278,** 21655–21662

9. Buzhynskyy, N., Salesse, C., and Scheuring, S. (2011) Rhodopsin is spatially heterogeneously distributed in rod outer segment disk membranes. *J. Mol. Recognit.* **24,** 483–489

10. Dell'Orco, D., and Koch, K.-W. (2011) A dynamic scaffolding mechanism for rhodopsin and transducin interaction in vertebrate vision. *Biochem. J.* **440,** 263–271

11. Salom, D., Lodowski, D. T., Stenkamp, R. E., Le Trong, I., Golczak, M., Jastrzebska, B., Harris, T., Ballesteros, J. A., and Palczewski, K. (2006) Crystal structure of a photoactivated deprotonated intermediate of rhodopsin. *Proc. Natl. Acad. Sci. U.S.A.* **103,** 16123–16128

12. Knepp, A. M., Periole, X., Marrink, S.-J., Sakmar, T. P., and Huber, T. (2012) Rhodopsin forms a dimer with cytoplasmic helix 8 contacts in native membranes. *Biochemistry* **51,** 1819–1821

13. Polozova, A., and Litman, B. J. (2000) Cholesterol dependent recruitment of di22:6-PC by a G protein-coupled receptor into lateral domains. *Biophys. J.* **79,** 2632–2643

14. Tanimoto, Y., Okada, K., Hayashi, F., and Morigaki, K. (2015) Evaluating the raftophilicity of rhodopsin photoreceptor in a patterned model membrane. *Biophys. J.* **109,** 2307–2316

15. Seno, K., Kishimoto, M., Abe, M., Higuchi, Y., Mieda, M., Owada, Y., Yoshiyama, W., Liu, H., and Hayashi, F. (2001) Light- and guanosine 5′-3-*O*-(thio)triphosphate-sensitive localization of a G protein and its effector on detergent-resistant membrane rafts in rod photoreceptor outer segments. *J. Biol. Chem.* **276,** 20813–20816

16. Jastrzebska, B., Ringler, P., Palczewski, K., and Engel, A. (2013) The rhodopsin-transducin complex houses two distinct rhodopsin molecules. *J. Struct. Biol.* **182,** 164–172

17. Palczewski, K. (2006) G protein-coupled receptor rhodopsin. *Annu. Rev. Biochem.* **75,** 743–767

18. Levental, I., Lingwood, D., Grzybek, M., Coskun, U., and Simons, K. (2010) Palmitoylation regulates raft affinity for the majority of integral raft proteins. *Proc. Natl. Acad. Sci. U.S.A.* **107,** 22050–22054

19. Gahbauer, S., and Böckmann, R. A. (2016) Membrane-mediated oligomerization of G protein coupled receptors and its implications for GPCR function. *Front. Physiol.* **7,** 494

20. Savi, P., Zachayus, J.-L., Delesque-Touchard, N., Labouret, C., Hervé, C., Uzabiaga, M.-F., Pereillo, J.-M., Culouscou, J.-M., Bono, F., Ferrara, P., and Herbert, J.-M. (2006) The active metabolite of clopidogrel disrupts P2Y12 receptor oligomers and partitions them out of lipid rafts. *Proc. Natl. Acad. Sci. U.S.A.* **103,** 11069–11074

21. MacKenzie, D., Arendt, A., Hargrave, P., McDowell, J. H., and Molday, R. S. (1984) Localization of binding sites for carboxyl terminal specific anti-rhodopsin monoclonal antibodies using synthetic peptides. *Biochemistry* **23,** 6544–6549

22. Nair, K. S., Balasubramanian, N., and Slepak, V. Z. (2002) Signal-dependent translocation of transducin, RGS9–1-Gβ5L complex, and arrestin to detergent-resistant membrane rafts in photoreceptors. *Curr. Biol.* **12,** 421–425

23. Martin, R. E., Elliott, M. H., Brush, R. S., and Anderson, R. E. (2005) Detailed characterization of the lipid composition of detergent-resistant membranes from photoreceptor rod outer segment membranes. *Invest. Ophthalmol. Vis. Sci.* **46,** 1147–1154

24. Jastrzebska, B., Golczak, M., Fotiadis, D., Engel, A., and Palczewski, K. (2009) Isolation and functional characterization of a stable complex between photoactivated rhodopsin and the G protein, transducin. *FASEB J.* **23,** 371–381

25. Jastrzebska, B., Debinski, A., Filipek, S., and Palczewski, K. (2011) Role of membrane integrity on G protein-coupled receptors: rhodopsin stability and function. *Prog. Lipid Res.* **50,** 267–277

26. Jastrzebska, B. (2015) Oligomeric state of rhodopsin within rhodopsin-transducin complex probed with succinylated concanavalin A. *Methods Mol. Biol.* **1271,** 221–233

27. Miljanich, G. P., Sklar, L. A., White, D. L., and Dratz, E. A. (1979) A disaturated and dipolyunsaturated phospholipids in the bovine retinal rod outer segment disk membrane. *Biochim. Biophys. Acta* **552,** 294–306

28. Kobe, F., Renner, U., Woehler, A., Wlodarczyk, J., Papusheva, E., Bao, G., Zeug, A., Richter, D. W., Neher, E., and Ponimaskin, E. (2008) Stimulation- and palmitoylation-dependent changes in oligomeric conformation of serotonin 5-HT1A receptors. *Biochim. Biophys. Acta* **1783,** 1503–1516

29. Zheng, H., Pearsall, E. A., Hurst, D. P., Zhang, Y., Chu, J., Zhou, Y., Reggio, P. H., Loh, H. H., and Law, P. (2012) Palmitoylation and membrane cholesterol stabilize μ-opioid receptor homodimerization and G protein coupling. *BMC Cell Biol.* **13,** 6

30. Ablonczy, Z., Kono, M., Knapp, D. R., and Crouch, R. K. (2006) Palmitoylation of cone opsins. *Vision Res.* **46,** 4493–4501

31. Schertler, G. F., Villa, C., and Henderson, R. (1993) Projection structure of rhodopsin. *Nature* **362,** 770–772

32. Ruprecht, J. J., Mielke, T., Vogel, R., Villa, C., and Schertler, G. F. (2004) Electron crystallography reveals the structure of metarhodopsin I. *EMBO J.* **23,** 3609–3620

33. Scheerer, P., Park, J. H., Hildebrand, P. W., Kim, Y. J., Krauss, N., Choe, H.-W., Hofmann, K. P., and Ernst, O. P. (2008) Crystal structure of opsin in its G-protein-interacting conformation. *Nature* **455,** 497–502

34. Choe, H.-W., Kim, Y. J., Park, J. H., Morizumi, T., Pai, E. F., Krauss, N., Hofmann, K. P., Scheerer, P., and Ernst, O. P. (2011) Crystal structure of metarhodopsin II. *Nature* **471,** 651–655

35. Dratz, E. A., Van Breemen, J. F., Kamps, K. M., Keegstra, W., and Van Bruggen, E. F. (1985) Two-dimensional crystallization of bovine rhodopsin. *Biochim. Biophys. Acta* **832,** 337–342

36. Mazzolini, M., Facchetti, G., Andolfi, L., Proietti Zaccaria, R., Tuccio, S., Treu, J., Altafini, C., Di Fabrizio, E. M., Lazzarino, M., Rapp, G., and Torre, V. (2015) The phototransduction machinery in the rod outer segment has a strong efficacy gradient. *Proc. Natl. Acad. Sci. U.S.A.* **112,** E2715–2724

37. Boesze-Battaglia, K., Fliesler, S. J., and Albert, A. D. (1990) Relationship of cholesterol content to spatial distribution and age of disk membranes in retinal rod outer segments. *J. Biol. Chem.* **265,** 18867–18870

38. Kawamura, S., and Tachibanaki, S. (2002) S-modulin. *Adv. Exp. Med. Biol.* **514,** 61–68

39. Wang, Z., Wen, X., Ablonczy, Z., Crouch, R. K., Makino, C. L., and Lem, J. (2005) Enhanced shutoff of phototransduction in transgenic mice expressing palmitoylation-deficient rhodopsin. *J. Biol. Chem.* **280,** 24293–24300

40. Senin, I. I., Höppner-Heitmann, D., Polkovnikova, O. O., Churumova, V. A., Tikhomirova, N. K., Philippov, P. P., and Koch, K.-W. (2004) Recoverin and rhodopsin kinase activity in detergent-resistant membrane rafts from rod outer segments. *J. Biol. Chem.* **279,** 48647–48653

41. Qanbar, R., and Bouvier, M. (2003) Role of palmitoylation/depalmitoylation reactions in G-protein-coupled receptor function. *Pharmacol. Ther.* **97,** 1–33

42. Yamazaki, A., Tatsumi, M., Torney, D. C., and Bitensky, M. W. (1987) The GTP-binding protein of rod outer segments. *J. Biol. Chem.* **262,** 9316–9323

43. Okada, T., Takeda, K., and Kouyama, T. (1998) Highly selective separation of rhodopsin from bovine rod outer segment membranes using combination of divalent cation and alkyl(thio)glucoside. *Photochem. Photobiol.* **67,** 495–499

44. Hayashi, F., and Yamazaki, A. (1991) Polymorphism in purified guanylate cyclase from vertebrate rod photoreceptors. *Proc. Natl. Acad. Sci. U.S.A.* **88,** 4746–4750

45. Wald, G., and Brown, P. K. (1953) The molar extinction of rhodopsin. *J. Gen. Physiol.* **37,** 189–200

46. Ernst, O. P., Gramse, V., Kolbe, M., Hofmann, K. P., and Heck, M. (2007) Monomeric G protein-coupled receptor rhodopsin in solution activates

its G protein transducin at the diffusion limit. *Proc. Natl. Acad. Sci. U.S.A.* **104,** 10859 –10864

47. Sachs, K., Maretzki, D., Meyer, C. K., and Hofmann, K. P. (2000) Diffusible ligand all-trans-retinal activates opsin via a palmitoylation-dependent mechanism. *J. Biol. Chem.* **275,** 6189 – 6194

48. Morrison, D. F., O'Brien, P. J., and Pepperberg, D. R. (1991) Depalmitoylation with hydroxylamine alters the functional properties of rhodopsin. *J. Biol. Chem.* **266,** 20118 –20123

49. Li, J., Edwards, P. C., Burghammer, M., Villa, C., and Schertler, G. F. (2004) Structure of bovine rhodopsin in a trigonal crystal form. *J. Mol. Biol.* **343,** 1409 –1438

50. Guex, N. and Peitsch, M.C. (1997) SWISS-MODEL and the Swiss-Pdb-Viewer: an environment for comparative protein modeling. *Electrophoresis* **18,** 2714 –2723

51. Gasteiger E., Gattiker A., Hoogland C., Ivanyi I., Appel R. D., and Bairoch, A. (2003) ExPASy: the proteomics server for in-depth protein knowledge and analysis. *Nucleic Acids Res.* **31,** 3784 –3788